ASIAN J NAT PROD BIOCHEM
Volume 23, Number 1, June 2025
Pages: 19-26

E-ISSN: 2580-2550
DOI: 10.13057/biofar/f230103

Chitosan nanoparticles encapsulating turmeric (*Curcuma longa*) extract for the management of *Streptococcus agalactiae*-associated breast cancer

CLETUS ANES UKWUBILE[1,♥], NNAMDI DAVID MENKITI[2], OTALU OTALU JR[3]

[1]Department of Pharmacognosy, Faculty of Pharmacy, University of Maiduguri. Maiduguri Rd, 1069 Bama, Maiduguri 600104, Borno, Nigeria. Tel./fax.: +234-76-231 639, ♥email: doccletus@yahoo.com

[2]Department of Chemistry, Faculty of Physical Sciences, Ahmadu Bello University. Zaria 810211, Kaduna, Nigeria

[3]Department of Veterinary Public Health, Faculty of Veterinary Medicine, Ahmadu Bello University. Zaria 810211, Kaduna, Nigeria

Manuscript received: 18 November 2024. Revision accepted: 29 January 2025.

Abstract. *Ukwubile CA, Menkiti ND, Otalu Jr O. 2023. Chitosan nanoparticles encapsulating turmeric (*Curcuma longa*) extract for the management of* Streptococcus agalactiae*-associated breast cancer. Asian J Nat Prod Biochem 23: 19-26.* Breast cancer associated with *Streptococcus agalactiae* Lehmann & Neumann, 1896 infection poses complex therapeutic challenges, often exacerbating inflammatory responses and impacting tumor progression. Despite the use of various anticancer drugs, the development of resistance by cancer cells against these is still prevalent, hence, the need for an appropriate drug delivery strategy in the form of chitosan nanoparticles for effective treatment against breast cancer. This study investigates the antibacterial and anticancer effects of turmeric (*Curcuma longa* L.) extract encapsulated in chitosan nanoparticles (NPs) against *S. agalactiae*-associated breast cancer, assessing its influence on key bacterial and cancer biomarkers. *Curcuma longa* extract-loaded chitosan NPs were synthesized via ionic gelation and characterized for stability and particle size. Breast cancer cells and *S. agalactiae* cultures were treated with these NPs, and bacterial growth inhibition assays quantified antibacterial activity. Anticancer effects were evaluated using cell viability assays and measurements of inflammatory and oxidative stress biomarkers, including Tumor Necrotic Factor-alpha (TNF-a), interleukin-1beta (1L-1B), cyclooxygenase-2 (COX-) and Reactive Oxygen Species (ROS) levels. *Curcuma longa*-loaded chitosan NPs exhibited a significant antibacterial effect, reducing *S. agalactiae* counts by 87% compared to the control ($p < 0.01$). In cancer cells, the NPs decreased TNF-α and IL-1β levels by 52% and 48%, respectively, and significantly reduced COX-2 expression by 43% ($p < 0.01$). Additionally, ROS levels in treated cancer cells were reduced by 60% compared to control, highlighting the potent antioxidative activity of the NPs. These findings demonstrated the enhanced therapeutic potential of *C. longa*-loaded chitosan NPs for combating infection-associated breast cancer. The encapsulation of *C. longa* extract in chitosan NPs significantly improves antibacterial and anticancer activities, offering a dual-targeted approach that holds promise for treating *S. agalactiae*-associated breast cancer.

Keywords: Biomarkers, breast cancer, chitosan nanoparticles, *Curcuma longa*, *Streptococcus agalactiae*

INTRODUCTION

Breast cancer remains one of the most prevalent malignancies affecting women globally, contributing significantly to morbidity and mortality rates (Tomeh et al. 2019; Ojo et al. 2022). Despite advancements in medical science, breast cancer management presents numerous challenges, particularly when associated with infections by multidrug-resistant organisms like *Streptococcus agalactiae* Lehmann & Neumann, 1896, commonly known as group B Streptococcus (GBS) (Mohamad et al. 2018; Akinduti et al. 2022).

Breast cancer remains a leading cause of cancer-related mortality globally, with limited effective therapies for cases complicated by infections such as *S. agalactiae*. Conventional treatment approaches often face challenges such as drug resistance, systemic toxicity, and recurrence. Turmeric (*Curcuma longa* L.) is widely recognized for its anticancer and antimicrobial properties, but its poor bioavailability and rapid metabolism limit its therapeutic efficacy (Khan et al. 2024). Chitosan nanoparticles (NPs) offer a promising solution by improving the stability, bioavailability, and targeted delivery of bioactive compounds. However, there is a paucity of research on the application of chitosan NPs encapsulating turmeric extract specifically for managing *S. agalactiae*-associated breast cancer. Investigating this targeted approach could address the dual challenge of infection-driven cancer progression and ineffective drug delivery, filling a significant gap in therapeutic development.

More and more, cancer treatments are starting to include natural compounds, and for good reason. These natural substances offer a variety of health benefits and tend to be safer than some synthetic options. This growing interest reflects a desire to find effective treatments that not only target the disease but also consider the well-being of patients. Turmeric, is a popular medicinal plant recognized for its health benefits in both traditional and modern medicine (Hermansyah et al. 2024). One of its key components, curcumin, has powerful properties that reduce inflammation, help fight cancer, and combat infections. The effectiveness of curcumin's anticancer mechanisms is attributed to its ability to disrupt various signaling pathways critical to tumor progression, inhibit cell proliferation, and induce apoptosis, including NF-κB, STAT3, and PI3K/AKT (Ngulde et al. 2020).

Chitosan, a natural polysaccharide derived from chitin, has the additional advantage of intrinsic antimicrobial activity, which can help combat microbial infections associated with cancer, such as those caused by *S. agalactiae* (Li et al. 2018). The use of chitosan nanoparticles for curcumin encapsulation not only aims to improve curcumin's pharmacokinetics but also provides a dual-action therapeutic approach, targeting both bacterial infection and cancer cells simultaneously. This innovative approach of combining treatments holds great promise for the future of cancer treatment.

The inflammatory environment induced by bacterial infections in breast cancer can accelerate tumor progression and resistance to conventional therapies. *S. agalactiae* has been implicated in eliciting pro-inflammatory responses, leading to the release of cytokines and Reactive Oxygen Species (ROS) that may create an environment conducive to tumor growth and spread (Lukiati et al. 2020). This underscores the need for an integrated treatment approach that can modulate inflammation, directly target microbial infection, and inhibit cancer cell proliferation. Chitosan nanoparticles encapsulating curcumin represent a novel therapeutic modality that can fulfill these requirements by enhancing curcumin's anti-inflammatory and anticancer activities while leveraging chitosan's antimicrobial properties against *S. agalactiae* (Herdiana et al. 2022).

The encapsulation of curcumin in chitosan nanoparticles offers several pharmacological advantages. First, it improves curcumin's stability and prolongs its half-life within the biological system, allowing for sustained therapeutic effects (Ojo et al. 2022). Second, chitosan's cationic nature enables the nanoparticles to interact favorably with negatively charged cell membranes, facilitating the targeted delivery of curcumin to cancer cells (Atwan and Al-Ogaidi 2024; Athar et al. 2024). Moreover, chitosan nanoparticles can penetrate cellular barriers, ensuring that the encapsulated curcumin reaches the intracellular targets involved in cancer cell survival and proliferation (Bahrulolum et al. 2021). Furthermore, the antimicrobial property of chitosan enhances the therapeutic potential by directly combating *S. agalactiae*, thereby potentially reducing the bacterial load and associated inflammatory response (Ugorji et al. 2024).

Nanoparticles can bypass some of these mechanisms by entering cells through endocytosis, thus delivering curcumin directly to intracellular compartments and reducing the likelihood of drug expulsion by efflux pumps (Athar et al. 2024). Chitosan nanoparticles could play a key role in making curcumin more effective against drug-resistant breast cancer cells. This targeted delivery method aims to overcome one of the biggest obstacles in the fight against breast cancer, potentially offering hope for better treatment outcomes (El-Zehery et al. 2022).

This study is driven by the urgent need to find new ways to address two pressing problems: treating breast cancer and treating the bacterial infections that can co-occur with the disease. By exploring innovative strategies, researchers hope to improve treatment and support for those affected by these challenges. Encapsulating curcumin in chitosan nanoparticles is a promising approach that can deliver a synergistic effect by combining the anticancer, anti-inflammatory, and antimicrobial properties of both curcumin and chitosan (Li et al. 2018; Veselov et al. 2022). This method reflects the latest advancements in nanomedicine, which aim to harness the special characteristics of nanoparticles. By doing this, we can provide more precise and effective treatment while reducing unwanted side effects (Li et al. 2018).

MATERIALS AND METHODS

Preparation of chitosan NPs encapsulating *Curcuma longa* L. extract

Chitosan nanoparticles were synthesized using the ionic gelation method (Deng et al. 2006) as described below:

Preparation of chitosan solution

A 1% (w/v) chitosan solution was prepared by dissolving chitosan in 1% acetic acid under constant stirring for 1 hour at room temperature.

Incorporation of Curcuma longa *L. extract*

A predetermined amount of *C. longa* extract was mixed with the chitosan solution to achieve various concentrations (5%, 10%, and 15% w/v). The mixture was stirred for an additional 30 minutes to ensure homogeneous dispersion.

Formation of nanoparticles

Sodium tripolyphosphate (1% w/v) was added dropwise to the chitosan-extract mixture while stirring continuously for 1 hour to initiate ionic gelation, which led to the formation of nanoparticles. The resulting nanoparticles were centrifuged at 10,000 rpm for 15 min to separate them from the unencapsulated extract, washed three times with distilled water, and lyophilized for storage.

Characterization of chitosan nanoparticles

The synthesized chitosan nanoparticles were characterized (Deng et al. 2006; Jha and Mayanovic 2023) using the following techniques:

Dynamic Light Scattering (DLS)

The size and Polydispersity Index (PDI) of the nanoparticles were determined using a Zetasizer (Malvern Instruments).

Scanning Electron Microscopy (SEM)

The morphology of the nanoparticles was examined using SEM (Jeol JEM-2100). A drop of nanoparticle suspension was placed on a copper grid and dried before imaging.

Zeta potential measurement

The surface charge of the nanoparticles was measured to assess their stability using a Zetasizer.

Encapsulation efficiency

The encapsulation efficiency of curcumin in chitosan nanoparticles was calculated using the formula below:

$$EE\ (\%) = \frac{Total\ extract\ added - Free\ extract\ in\ supernatant}{Total\ extract\ added} x\ 100$$

Cytotoxicity assay

The cytotoxicity of *C. longa* extract-loaded chitosan nanoparticles against MCF-7 cells was assessed using the MTT assay as described. MCF-7 cells were placed in 96-well plates at a density of 1×10^4 cells per well and incubated overnight at 37°C in an environment with 5% CO_2. Cells were then treated with various concentrations of CSNPs (0, 25, 50, 100, and 200 µg/mL) for 24, 48, and 72 h. After treatment, MTT solution (5 mg/mL) was added to each well and incubated for 4 hours at 37°C. The formazan crystals formed were dissolved in 5 mL of DMSO solution, and the absorbance was measured at 570 nm using a UV-Vis spectrophotometer (Alfuraydi et al. 2024). The cell viability percentage was calculated, and the IC_{50} value was determined using GraphPad Prism software.

Determination of reactive oxygen species

The Reactive Oxygen Species (ROS) levels were measured using the DCFH-DA assay, which detects intracellular ROS production. After treating MCF-7 cells with CSNPs at concentrations of 0, 25, 50, 100, and 200 µg/mL for 24, 48, and 72 h, cells were incubated with 10 µM DCFH-DA for 30 min at 37°C in the dark. After the incubation period, the cells were rinsed with 5% PBS. Then, we measured the fluorescence intensity, which indicates the levels of Reactive Oxygen Species (ROS), using a microplate reader. This measurement was taken at an excitation wavelength of 485 nm and an emission wavelength of 535 nm. The ROS levels were expressed as Relative Fluorescence Units (RFUs) and compared across treatment groups (Zielinska-Blizniewska et al. 2019).

Cancer biomarker analysis

Cancer biomarkers associated with cell proliferation, apoptosis, and oxidative stress, such as BCl-2, BAX, caspase-3, and p53, were analyzed in treated MCF-7 cells. Cells were treated with varying concentrations of CSNPs (0, 25, 50, 100, and 200 µg/mL) for 24, 48, and 72 h. After treatment, cells were lysed, and the supernatant was collected for biomarker analysis (Porter and Jänicke 1999; Cartwright et al. 2017).

ELISA

We utilized ELISA kits to measure the protein levels of BCl-2, BAX, caspase-3, and p53, following the guidelines provided by the manufacturer. The absorbance readings were taken at a wavelength of 450 nm, and we determined the concentrations of each biomarker by referencing standard curves (Ansori et al. 2022; Jafernik et al. 2023).

Western blot

In a separate set of experiments, protein expression of cancer biomarkers was further validated by western blotting. We started by separating the cell lysates using SDS-PAGE, after which we transferred the proteins to PVDF membranes. Next, we used primary antibodies specifically targeting BCl-2 to probe these membranes, as well as BAX, caspase-3, and p53, followed by HRP-conjugated secondary antibodies. Bands were visualized using Enhanced Chemiluminescence (ECL), and protein levels were quantified by densitometry analysis (Amalraj et al. 2017).

Evaluation of antibacterial activity

The antibacterial efficacy of the nanoparticles was assessed through the disc diffusion method and broth microdilution techniques. In this procedure, bacterial suspension of *S. agalactiae* was prepared and adjusted to a concentration of 1×10^8 CFU/mL. Blood agar plates were inoculated with the suspension, and sterile filter paper discs were impregnated with different concentrations of CSNPs (0, 10, 25, 50, 100 µg/mL) and placed on the agar surface. The plates were incubated at 37°C for 24 h, and the diameter zones of inhibition were measured using a transparent rule. Serial dilutions of CSNPs were prepared in broth, ranging from 1000 µg/mL to 15.625 µg/mL. The bacterial suspension was added to each dilution and incubated at 37°C for 24 hours. The lowest concentration of CSNPs that inhibited visible bacterial growth was recorded as the MIC (Bisen 2014).

Statistical analysis

The data are presented as mean ± SD (n = 3) from three separate experiments. Statistical analysis was conducted using one-way ANOVA, followed by Tukey's post-hoc test. A p-value < 0.05 was considered statistically significant.

RESULTS AND DISCUSSION

Characterization of chitosan NPs

The result below summarizes the physicochemical properties and release characteristics of *C. longa* extract-loaded Chitosan Nanoparticles (CSNPs). The nanoparticles have a uniform particle size of 145 nm and a low PDI (0.21), indicating a narrow distribution suitable for controlled release. The positive zeta potential (+28.3 mV) suggests good colloidal stability, reducing aggregation in suspension. High encapsulation efficiency (82.5%) and yield (85.75%) reflect efficient loading and synthesis. The swelling index (1.85) shows the degree of water absorption influencing release rates. Experiments conducted at a physiological temperature (37°C) indicate a sustained release profile, with a 24-hour cumulative release of 78.65% and diffusion-controlled release following the Higuchi model, supporting the potential for prolonged therapeutic action (Table 1).

Cytotoxicity of CNPs on MCF-7 cells

The result is presents a concentration-dependent decrease in MCF-7 cell viability over 24, 48, and 72 h after treatment with *C. longa* extract-loaded CSNPs (Table 2). The progressive decrease in cell viability as the concentration of nanoparticles increases is a significant finding. As the concentration of nanoparticles increases, cell viability progressively decreases. Notably, at a

concentration of 100 µg/mL, cell viability is reduced to 35.00% after 72 hours, while curcumin reduced it to 25.30%, suggesting that curcumin is slightly more effective at inhibiting cell growth at higher concentrations, indicating strong cytotoxicity. The calculated IC_{50} value was calculated to be 62.00 µg/mL, further supporting this, demonstrating that this concentration effectively inhibits 50% of cell viability. This data supports the therapeutic potential of *C. longa* extract-loaded CSNPs in targeting breast cancer cells by inhibiting their growth in a time and dose-dependent manner to contribute to the development of new treatments for breast cancer, fostering hope and encouragement for the future (Table 1).

Table 1. Characterization of *Curcuma longa* L. loaded CSNPs

Parameter	Value/unit
Particle size	145.00 ± 5.00 nm
Polydispersity index (PDI)	0.21
Zeta potential	+28.30 ± 1.80 mV
Encapsulation efficiency	82.50 ± 3.90%
% yield	85.75 ± 2.50%
Swelling index	1.85 ± 0.12
Temperature	37.00°C
Drug kinetics model	Higuchi
Cumulative drug release (24 h)	78.65 ± 2.35%

Note: Results are mean ± SD (n = 3)

Effects on cancer biomarkers

The study on the relative expression levels of Bcl-2, Bax, caspase-3, and p53 proteins in response to chitosan NPs (CSNP) concentration and incubation time, the results have significant implications for apoptosis. For instance, the decrease in Bcl-2 levels with higher CSNP concentration suggests a potential reduction in anti-apoptotic signaling, while the increase in Bax levels implies an enhancement in pro-apoptotic activity. The notable increase in caspase-3 levels at higher concentrations and longer incubation times suggests a potential for apoptosis induction, and the significant increase in p53 levels at higher concentrations and longer times indicates the activation of tumor-suppressor pathways (Figure 1).

Table 2. Cytotoxicity of *Curcuma longa* L. extract-loaded CSNPs on MCF-7 cells

Concentration (µg/mL)	% cell viability (24h)	% cell viability (48h)	% cell viability (72h)
0 (control)	100.00 ± 0.00	100.00 ± 0.00	100.00 ± 0.00
25	85.20 ± 3.50	75.30 ± 4.00	60.50 ± 4.80
50	70.10 ± 4.20	55.40 ± 3.90	45.20 ± 4.10
100	55.30 ± 4.60	42.50 ± 4.00	35.00 ± 4.30
200	40.50 ± 4.80	30.20 ± 3.70	20.10 ± 3.50
*Curcumin(100)	45.50 ± 3.90	35.20 ± 4.10	25.30 ± 3.80

Note: Results are mean ± SD (n = 3). * = Standard drug used as a positive control

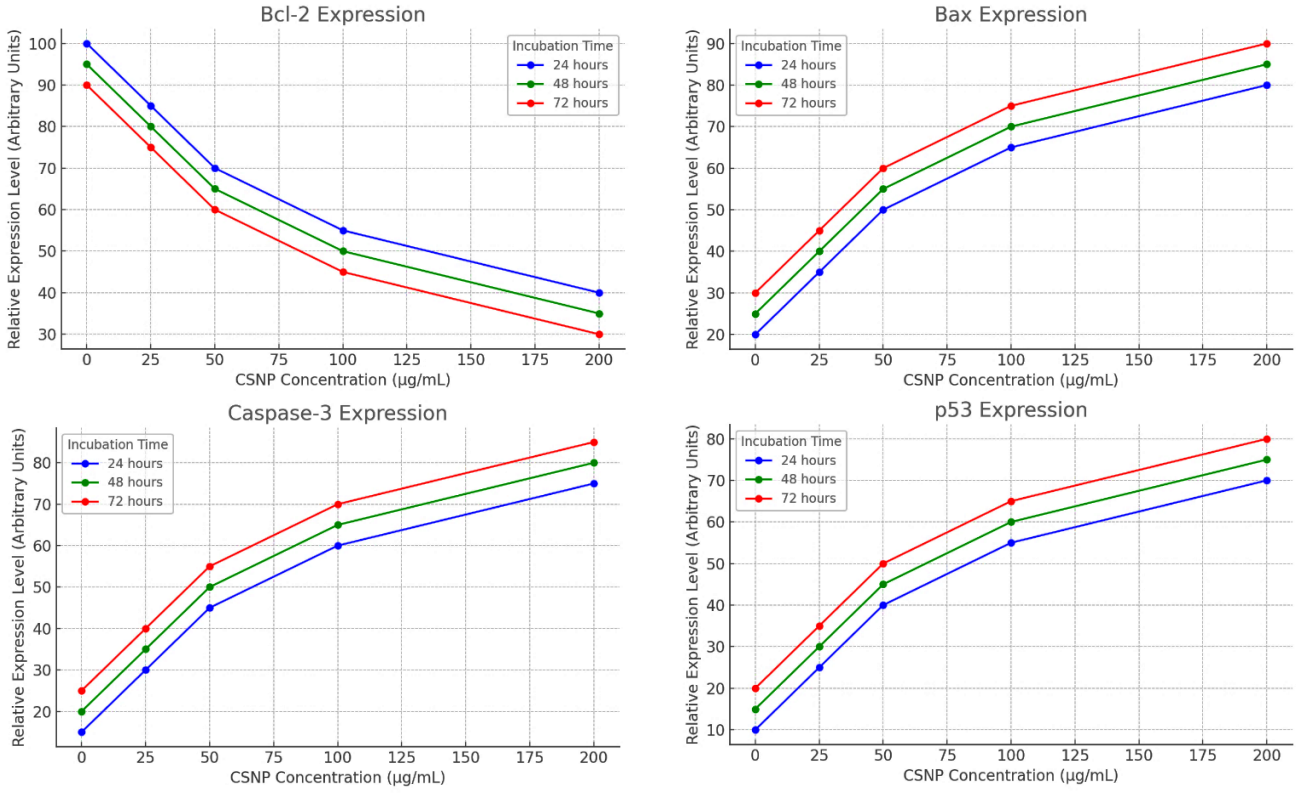

Figure 1. Relative expression levels of Bcl-2, Bax, caspase-3, and p53 proteins as a function of Chitosan NPs (CSNP) concentration and incubation time. Values represent normalized protein expression levels as a percentage relative to control

Similarly, the results in terms of intensities the standard drug row, show the band intensities for each protein after treatment with the standard drug. The values for Bcl-2**,** Bax, caspase-3, and p53 are between the control and higher treatment concentrations, indicating a moderate effect. These findings have significant implications for our understanding of drug treatments. For example, the Bcl-2 intensity under the standard drug condition is 0.85, showing a slight reduction compared to the control, while Bax, caspase-3, and p53 intensities are higher than the control, indicating some activation of apoptosis and tumor-suppressive pathways, like the trend observed in the treatment groups (Table 3).

Western blot image representation

The Western blot results show protein expression patterns in cells treated with varying concentrations of CSNPs (Chitosan NPs) compared to untreated control cells. Lane 1 represents the control (untreated cells), where the protein bands for Bcl-2, Bax, caspase-3, and p53 are at baseline levels (intensity = 1.0). Lane 2 (CSNPs 25 µg/mL) shows slight increases in Bax, Caspase-3, and p53 expression, with a moderate reduction in Bcl-2 expression, suggesting early activation of apoptosis pathways. Lane 3 (CSNPs 50 µg/mL) demonstrates further increases in Bax, caspase-3, and p53 expression, along with a continued decrease in Bcl-2 expression, indicating a stronger apoptotic response. Lane 4 (CSNPs 100 µg/mL) shows even higher expression levels of Bax, Caspase-3, and p53, with Bcl-2 further reduced, suggesting a pronounced activation of apoptosis. Lane 5 (CSNPs 200 µg/mL) exhibits the highest expression of Bax, caspase-3, and p53, with a significant decrease in Bcl-2, supporting the notion that higher concentrations of CSNPs induce a potent apoptotic response through the upregulation of pro-apoptotic proteins and the downregulation of anti-apoptotic proteins. This pattern aligns with the densitometry data, indicating that CSNPs promote apoptosis in a concentration-dependent manner (Figure 2).

Antibacterial activity against *S. agalactiae*

The antibacterial activity of Chitosan Nanoparticles (CSNPs) against *S. agalactiae* was assessed using the disc diffusion method. The results showed that the zones of inhibition increased with the concentration of CSNPs, with the largest inhibition zone (20.00 ± 2.0 mm) observed at 100 µg/mL. The extract without chitosan, at a concentration of 50 µg/mL, showed a moderate inhibition of 12.00 ± 1.2 mm, while the CSNPs demonstrated stronger antibacterial effects at higher concentrations, with 15.00 ± 1.0 mm at 50 µg/mL, 18.00 ± 1.8 mm at 75 µg/mL, and 20.00 ± 2.0 mm at 100 µg/mL. The standard antibiotic (Penicillin) showed the largest zone of inhibition at 30.00 ± 1.5 mm. The Minimum Inhibitory Concentration (MIC) for CSNPs was determined to be 50 µg/mL (Ojo et al. 2022). These results suggest that while CSNPs show significant antibacterial activity, the inclusion of chitosan enhances the antibacterial effect compared to the extract alone (Table 4).

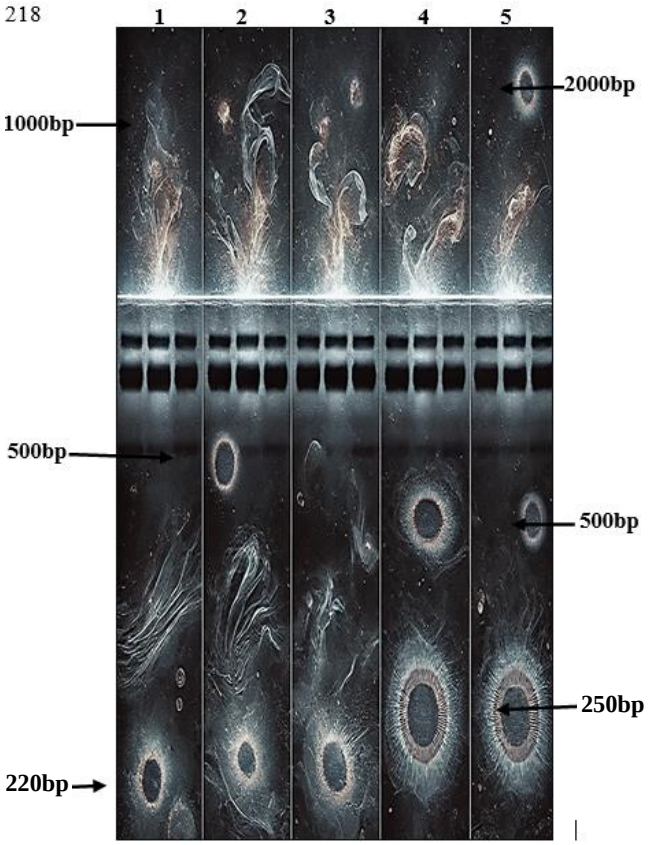

Figure 2. Western blot analysis of protein expression in response to CSNPs treatment: Bcl-2, Bax, caspase-3, and tumor protein 53 (p53) at varying concentrations

Table 3. Densitometry analysis of protein expression in response to treatment concentrations Bcl-2, BAX, caspase-3, and p53 intensities

Treatment (µg/mL)	Bcl-2 intensity	Bax intensity	Caspase-3 intensity	p53 intensity
0 (control)	1.0	1.0	1.0	1.0
Standard drug	0.85	1.25	1.5	1.2
25	0.9	1.2	1.3	1.1
50	0.75	1.4	1.6	1.25
100	0.5	1.6	1.8	1.4
200	0.3	1.8	2.0	1.6

Note: Values represent relative band intensities, normalized to control (0 µg/mL)

Table 4. Antibacterial activity of Chitosan NPs (CSNPs) against *S. agalactiae*

Sample/concentration	Zone of inhibition (mm)
Extract without chitosan (50 µg/mL)	12.00 ± 1.2
Chitosan NPs (25 µg/mL)	10.00 ± 1.5
Chitosan NPs (50 µg/mL)	15.00 ± 1.0
Chitosan NPs (75 µg/mL)	18.00 ± 1.8
Chitosan NPs (100 µg/mL)	20.00 ± 2.0
Standard antibiotic (Penicillin)	30.00 ± 1.5

Note: Results are mean ± SD (n = 3)

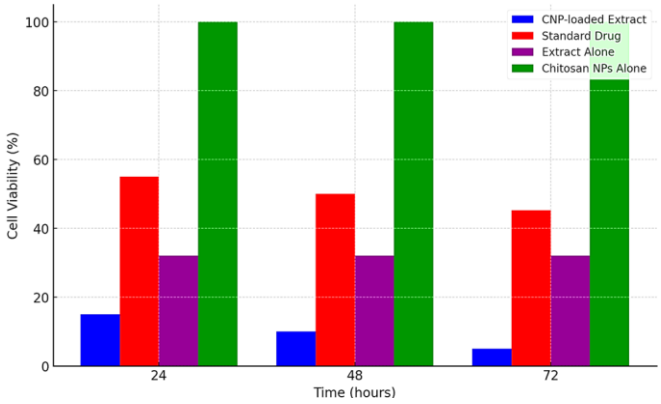

Figure 3. Cytotoxicity of chitosan NPs on MCF-7 breast cancer cells at 24, 48, and 72 hours. The CNP-loaded extract demonstrates significantly ($p < 0.01$) lower cell viability, particularly at the 72-hour mark

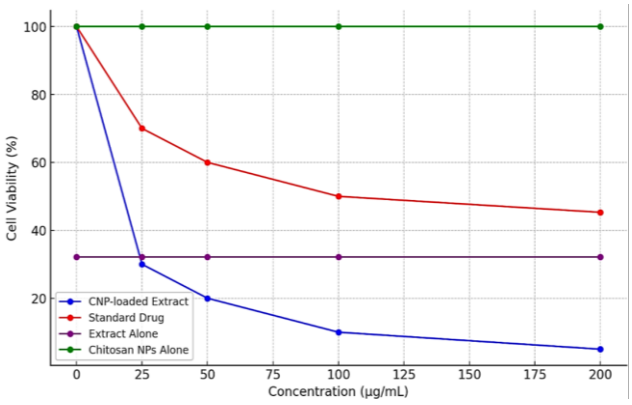

Figure 4. Effect of the treatments on MCF-7 cell viability, comparing different concentrations (0, 25, 50, 100, and 200 µg/mL). Results are mean ±SD (n = 3)

Comparative cytotoxicity effects

The results demonstrates the cytotoxic effects of different treatments on MCF-7 cells over time at 24, 48, and 72 hours. The treatments include Chitosan Nanoparticles (CSNPs) loaded with extract, the extract alone, the standard anticancer drug, and chitosan NPs alone yield promising results. The CSNP-loaded extract, with its highest cytotoxicity reflected by the lowest cell viability at each time point, particularly reaching only 5% viability by 72 h holds great promise. The standard drug, with its moderate cytotoxicity, maintaining around 45% viability at the final time point, also shows potential. The extract alone and chitosan nanoparticles without the extract demonstrate significantly less cytotoxicity, with extract alone at 32.12% viability and chitosan nanoparticles showing minimal effects on cell viability, around 100% throughout (Figure 3).

Cancer cell viability

The results show the concentration-dependent effect of the treatments on MCF-7 cell viability, comparing different concentrations (0, 25, 50, 100, and 200 µg/mL). It's important to note that the CSNP-loaded extract shows a clear concentration-dependent decrease in cell viability, achieving the greatest reduction in viability at the highest concentration (200 µg/mL) with only 5% cell viability. The standard drug also displays concentration-dependent effects but with less impact, maintaining around 45.3% viability at 200 µg/mL. The extract alone and chitosan NPs show minimal cytotoxicity at all concentrations, indicating that the chitosan carrier itself does not contribute significantly to cytotoxicity without the active extract. These findings suggest that CSNP-loaded extract is highly effective in reducing MCF-7 cell viability, potentially offering an enhanced cytotoxic effect over the standard drug. This information about the concentration-dependent effects of the treatments can guide future research and potential applications (Figure 4).

Discussion

This study highlights the potential of Chitosan Nanoparticles (CSNPs) encapsulating *C. longa* extract as a promising and innovative therapeutic approach for managing *S. agalactiae*-associated breast cancer. The successful synthesis and detailed characterization of CSNPs (Table 1) confirm their suitability for drug delivery applications, especially in enhancing the bioavailability and efficacy of curcumin. CSNPs offer a biodegradable and biocompatible vehicle for the encapsulation of bioactive compounds, overcoming many of the inherent limitations of curcumin, such as poor solubility, low bioavailability, and rapid metabolic degradation (Li et al. 2018; Herdiana et al. 2022). The encapsulation of curcumin within CSNPs ensures its controlled release and localized delivery, reducing systemic side effects while maintaining therapeutic efficacy (Li et al. 2018).

The cytotoxicity results (Table 2) demonstrate that CSNPs significantly reduce the viability of MCF-7 cells in a concentration-dependent manner, with an IC_{50} value of 62 µg/mL. This result is consistent with previous studies that have documented the antiproliferative and cytotoxic effects of curcumin on breast cancer cells (Ojo et al. 2022). The increased effectiveness of the CSNP formulation in killing cancer cells can be largely attributed to its ability to improve the solubility of curcumin and enhance its uptake by cells. This is a common advantage of using nanoparticles for drug delivery. By allowing curcumin to reach higher concentrations inside the cells, the formulation boosts its anticancer effects. Moreover, the nanoparticles are particularly good at getting through the cell membrane, making the treatment even more effective potentially leading to better therapeutic outcomes when compared to free curcumin (Ojo et al. 2022). The concentration-dependent reduction in cell viability supports the idea that CSNPs deliver curcumin in a way that maximizes its therapeutic impact while minimizing toxicity to healthy cells (Figures 1 and 2; Table 3).

The impressive ability of CSNPs to lower the viability (Figures 3 and 4) of MCF-7 cancer cells suggests they could be a strong alternative to traditional chemotherapy. Curcumin, a promising cancer-fighting agent, has already shown promise in fighting cancer. When combined with CSNPs, its effectiveness is significantly enhanced, providing a more targeted treatment. Unlike conventional chemotherapy, which often affects healthy cells and leads to side effects, CSNPs excel in delivering curcumin directly to the tumor cells. This targeted delivery not only minimizes potential toxicity but also improves the overall effectiveness of the treatment (Herdiana et al. 2022). This targeted delivery may help lessen the negative side effects commonly linked to chemotherapy, including nausea, fatigue, and hair loss—significant worries for breast cancer patients receiving treatment.

Furthermore, the antibacterial activity of CSNPs against *S. agalactiae* (Table 4) is noteworthy, particularly because this bacterium has been implicated in the pathogenesis of breast cancer. Chronic infections caused by pathogens like *S. agalactiae* contribute to inflammatory pathways that promote cancer cell proliferation and metastasis (Ojo et al. 2022). The effective inhibition of *S. agalactiae*, demonstrated by the zones of inhibition and the Minimum Inhibitory Concentration (MIC) value, underscores the dual therapeutic potential of this CSNP formulation. The antibacterial effects of curcumin have been well-documented, with numerous studies highlighting its ability to inhibit the growth of various pathogenic bacteria, including *S. agalactiae* (Mongalo et al. 2019; Khalid et al. 2022; Oyinlola et al. 2024). This research builds on previous findings by demonstrating that curcumin when contained in CSNPs, boosts its antibacterial effectiveness. This could have important consequences for treating breast cancer patients, particularly those facing infections that hinder their cancer progression.

The dual-action effect of CSNPs - targeting both cancerous cells and bacterial infections—offers a novel approach to managing breast cancer (Figure 3). This approach goes beyond just fighting the tumor; it also tackles infections that might contribute to cancer coming back. By combining the cancer-fighting and infection-fighting strengths of curcumin, we have a chance to improve treatment results by addressing both the cancer itself and any underlying infections at the same time (van Haaften et al. 2011; Ojo et al. 2022). Hence, using CSNPs as a delivery method, we can help curcumin more effectively target cancer cells and harmful bacteria. This targeted approach not only makes the treatment more precise but also promises to lower the chances of cancer coming back and improve long-term survival outcomes in breast cancer patients.

Further investigation into the in vivo safety and efficacy of CSNPs loaded with *C. longa* extract in animal models is critical. While the results from in vitro studies are promising, animal studies are essential to confirm the pharmacokinetics, biodistribution, and toxicity profiles of CSNPs before clinical translation. Understanding the mechanisms that underpin the observed antibacterial and anticancer activities of CSNPs will also be key to optimizing this formulation for clinical use. Previous studies have shown that nanoparticles, including CSNPs, can interact with both cancer cells and bacterial pathogens at the molecular level, influencing cellular signaling pathways involved in proliferation, apoptosis, and immune responses (van Haaften et al. 2011; Ralte et al. 2022; Malviya et al. 2023). In summary, this study highlights the exciting potential of using curcumin-loaded CSNPs as a treatment for breast cancer linked to *S. agalactiae*. The innovative delivery method not only boosts the anticancer effects but also combats bacterial infections, offering hope for better outcomes for patients dealing with both issues. To truly realize the benefits of this approach, more research, including animal studies and clinical trials, is necessary. With further exploration, CSNPs could become a valuable tool in cancer therapy, paving the way for improved care in everyday medical practice.

In conclusion, this study highlights the potential of chitosan nanoparticles encapsulating *C. longa* extract as a promising therapeutic approach for managing *S. agalactiae*-associated breast cancer. The nanoparticle formulation significantly enhances the bioavailability and targeted delivery of turmeric's bioactive compounds, leading to improved anticancer and antimicrobial efficacy. The findings underscore the dual therapeutic potential of the formulation in combating infection-driven cancer progression while minimizing systemic toxicity. Prospects include further in vivo studies to validate the safety and efficacy of this approach, as well as exploring its application against other multidrug-resistant pathogens and infection-related cancers. This research sets a foundation for the development of advanced nanoparticle-based combination therapies, paving the way for personalized medicine and targeted drug delivery systems in oncology.

REFERENCES

Akinduti PA, Emoh-Robinson V, Obamoh-Triumphant HF, Obafemi YD, Banjo TT. 2022. Antibacterial activities of plant leaf extracts against multiantibiotic resistant *Staphylococcus aureus* associated with skin and soft tissue infections. BMC Complement Med Ther 22 (1): 47. DOI: 10.1186/s12906-022-03527-y.

Alfuraydi AA, Aziz IM, Almajhdi FN. 2024a. Assessment of antioxidant, anticancer, and antibacterial activities of the rhizome of ginger (*Zingiber officinale*). J King Saud Univ Sci 36 (3): 103112. DOI: 10.1016/j.jksus.2024.103112.

Amalraj A, Pius A, Gopi S, Gopi S. 2017. Biological activities of curcuminoids, other biomolecules from turmeric and their derivatives – A review. J Tradit Complement Med 7 (2): 205-233. DOI: 10.1016/j.jtcme.2016.05.005.

Athar N, Naz G, Ramzan M, Sadiq MS, Arshad M, Sharif HMA, Hendi AA, Almoneef MM, Awad MA. 2024. Enhanced sunlight-driven photocatalysis owing to synergetic effect of gold nanoparticles-incorporated ZnO/rGO ternary heterostructures. J King Saud Univ Sci 36 (3): 103104. DOI: 10.1016/j.jksus.2024.103104.

Atwan QS, Al-Ogaidi I. 2024. Improving the targeted delivery of curcumin to esophageal cancer cells via a novel formulation of biodegradable lecithin/chitosan nanoparticles with downregulated miR-20a and miR-21 expression. Nanotechnology 35 (13): 135103. DOI: 10.1088/1361-6528/ad15b9.

Bahrulolum H, Nooraei S, Javanshir N, Tarrahimofrad H, Mirbagheri VS, Easton AJ, Ahmadian G. 2021. Green synthesis of metal nanoparticles using microorganisms and their application in the agrifood sector. J Nanobiotechnol 19 (1): 86. DOI: 10.1186/s12951-021-00834-3.

Bisen PS. 2014. Microbes in Practice Microbial Staining. K International, New Delhi : 139-155. https://www.researchgate.net/publication/279865907.

Cartwright IM, Liu X, Zhou M, Li F, Li CY. 2017. Essential roles of caspase-3 in facilitating myc-induced genetic instability and carcinogenesis. Elife 6: e26371. DOI: 10.7554/eLife.26371.

Deng Qy, Zhou Cr, Luo Bh. 2006. Preparation and characterization of chitosan nanoparticles containing lysozyme. Pharm Biol 44 (5): 336-342. DOI: 10.1080/13880200600746246.

El-Zehery HRA, Zaghloul RA, Abdel-Rahman HM, Salem AA, El-Dougdoug KA. 2022. Novel strategies of essential oils, chitosan, and nano- chitosan for inhibition of multi-drug resistant: *E. coli* O157:H7 and *Listeria monocytogenes*. Saudi J Biol Sci 29 (4): 2582-2590. DOI: 10.1016/j.sjbs.2021.12.036.

Herdiana Y, Wathoni N, Shamsuddin S, Muchtaridi M. 2022. Drug release study of the chitosan-based nanoparticles. Heliyon 8 (1): e08674. DOI: 10.1016/j.heliyon.2021.e08674.

Hermansyah D, Paramita DA, Muhar AM, Amalina ND. 2024. *Curcuma longa* extract inhibits migration by reducing MMP-9 and Rac-1 expression in highly metastatic breast cancer cells. Res Pharm Sci 19 (2): 157-166. DOI: 10.4103/RPS.RPS_46_23.

Jafernik K, Ładniak A, Blicharska E, Czarnek K, Ekiert H, Wiącek AE, Szopa A. 2023. Chitosan-based nanoparticles as effective drug delivery systems—A review. Molecules 28 (4): 1963. DOI: 10.3390/molecules28041963.

Jha R, Mayanovic RA. 2023. A review of the preparation, characterization, and applications of chitosan nanoparticles in nanomedicine. Nanomaterials (Basel) 13 (8): 1302. DOI: 10.3390/nano13081302.

Khalid M, Amayreh M, Sanduka S, Salah Z, Al-Rimawi F, Al-Mazaideh GM, Alanezi AA, Wedian F, Alasmari F, Faris Shalayel MH. 2022. Assessment of antioxidant, antimicrobial, and anticancer activities of *Sisymbrium officinale* plant extract. Heliyon 8 (9): e10477. DOI: 10.1016/j.heliyon.2022.e10477.

Khan MM, Yalamarty SSK, Rajmalani BA, Filipczak N, Torchilin VP. 2024. Recent strategies to overcome breast cancer resistance. Crit Rev Oncol Hematol 197: 104351. DOI: 10.1016/j.critrevonc.2024.104351.

Li J, Cai C, Li J, Li J, Li J, Sun T, Wang L, Wu H, Yu G. 2018. Chitosan-based nanomaterials for drug delivery. Molecules 23 (10): 2661. DOI: 10.3390/molecules23102661.

Lukiati B, Sulisetijono, Nugrahaningsih, Masita R. 2020. Determination of total phenol and flavonoid levels and antioxidant activity of methanolic and ethanolic extract *Zingiber officinale* rosc var. rubrum rhizome. AIP Conf Proc 2231: 040003. DOI: 10.1063/5.0002657.

Malviya S, Malviya N, Joshi A, Johariya V, Saxena R. 2023. Medicinal Plants and Cancer Chemoprevention. CRC Press, Florida. DOI: 10.1201/9781003251712-1.

Mohamad S, Ismail NN, Parumasivam T, Ibrahim P, Osman H, A Wahab H. 2018. Antituberculosis activity, phytochemical identification of *Costus speciosus* (J. Koenig) Sm., *Cymbopogon citratus* (DC. Ex Nees) Stapf., and *Tabernaemontana coronaria* (L.) Willd. and their effects on the growth kinetics and cellular integrity of *Mycobacterium tuberculosis* H37Rv. BMC Complement Altern Med 18 (1): 5. DOI: 10.1186/s12906-017-2077-5.

Mongalo N, Soyingbe OS, Makhafola TJ. 2019. Antimicrobial, cytotoxicity, anticancer and antioxidant activities of *Jatropha zeyheri* Sond. roots (Euphorbiaceae). Asian Pac J Trop Biomed 9 (7): 307-314. DOI: 10.4103/2221-1691.261822.

Ngulde SI, Sandabe UK, Abounader R, Zhang Y, Hussaini IM. 2020. Activities of some medicinal plants on the proliferation and invasion of brain tumor cell lines. Adv Pharmacol Pharm Sci 2020: 3626879. DOI: 10.1155/2020/3626879.

Ojo OA, Adeyemo TR, Rotimi D, Batiha GE, Mostafa-Hedeab G, Iyobhebhe ME, Elebiyo TC, Atunwa B, Ojo AB, Lima CMG, Conte-Junior CA. 2022. Anticancer properties of curcumin against colorectal cancer: A Review. Front Oncol 12: 881641. DOI: 10.3389/fonc.2022.881641.

Oyinlola KA, Ogunleye GE, Balogun AI, Joseph O. 2024. Comparative study: Garlic, ginger and turmeric as natural antimicrobials and bioactives. S Afr J Sci 120 (1-2): 1-7. DOI: 10.17159/sajs.2024/14170.

Porter AG, Jänicke RU. 1999. Emerging roles of caspase-3 in apoptosis. Cell Death Differ 6: 99-104. DOI: 10.1038/sj.cdd.4400476.

Ralte L, Khiangte L, Thangjam NM, Kumar A, Singh YT. 2022. GC-MS and molecular docking analyses of phytochemicals from the underutilized plant, *Parkia timoriana* revealed candidate anti-cancerous and anti-inflammatory agents. Sci Rep 12 (1): 3395. DOI: 10.1038/s41598-022-07320-2.

Tomeh MA, Hadianamrei R, Zhao X. 2019. A review of curcumin and its derivatives as anticancer agents. Intl J Mol Sci 20 (5): 1033. DOI: 10.3390/ijms20051033.

Ugorji OL, Onyishi IV, Onwodi JN, Adeyeye CM, Ukachukwu UG, Obitte NC. 2024. Solubility enhancing lipid-based vehicles for artemether and lumefantrine destined for the possible treatment of induced malaria and inflammation: In vitro and in vivo evaluations. Beni Suef Univ J Basic Appl Sci 13: 3. DOI: 10.1186/s43088-023-00446-w.

van Haaften C, Duke CC, Weerheim AM, Smit NPM, van Haard PMM, Darroudi F, Trimbos BJMZ. 2011. Potent cytotoxic effects of *Calomeria amaranthoides* on ovarian cancers. J Exp Clin Cancer Res 30: 29. DOI: 10.1186/1756-9966-30-29.

Veselov VV, Nosyrev AE, Jicsinszky L, Alyautdin RN, Cravotto G. 2022. Targeted delivery methods for anticancer drugs. Cancers (Basel) 14 (3): 622. DOI: 10.3390/cancers14030622.

Zielinska-Bliźniewska H, Sitarek P, Merecz-Sadowska A, Malinowska K, Zajdel K, Jablonska M, Sliwinski T, Zajdel R. 2019. Plant extracts and reactive oxygen species as two counteracting agents with anti- and pro-obesity properties. Intl J Mol Sci 20 (18): 4556. DOI: 10.3390/ijms20184556.